Supplementally Information:

Molecular insight of visible light driven photocatalytic hydrogen peroxide synthesis using heptazine-imide structure

Yamato Yamanaka[a], Kohei Sawada[b], Mizuki Nanke[a], Xiao-Feng Shen[c], Jun-Tae Song[a,c], Tatsuki Abe[d], Keiji Tanaka[a,b,c,d], Toshinori Matsushima[a,b,c,e], Miki Inada[a,c], Tatsumi Ishihara[a,b,c,e] and Motonori Watanabe[a,b,c,e]*

[a.] *Department of Applied Chemistry, Graduate School of Engineering, Kyushu University, 744 Motooka, Nishi-ku, Fukuoka, 8190385, Japan*
[b.] *Department of Automotive Science, Graduate School of Integrated Frontier Sciences, Kyushu University, 744 Motooka, Nishi-ku, Fukuoka, 8190385, Japan*
[c.] *International Institute for Carbon Neutral Research (I²CNER), Kyushu University, 744 Motooka, Nishi-ku, Fukuoka, 8190385, Japan*
[d.] *Center for Polymer Interface and Molecular Adhesion Science, Kyushu University, 744 Motooka, Nishi-ku, Fukuoka, 8190385, Japan*
[e.] *Center for Energy Systems Design (CESD), Kyushu University, 744 Motooka, Nishi-ku, Fukuoka 8190395, Japan*

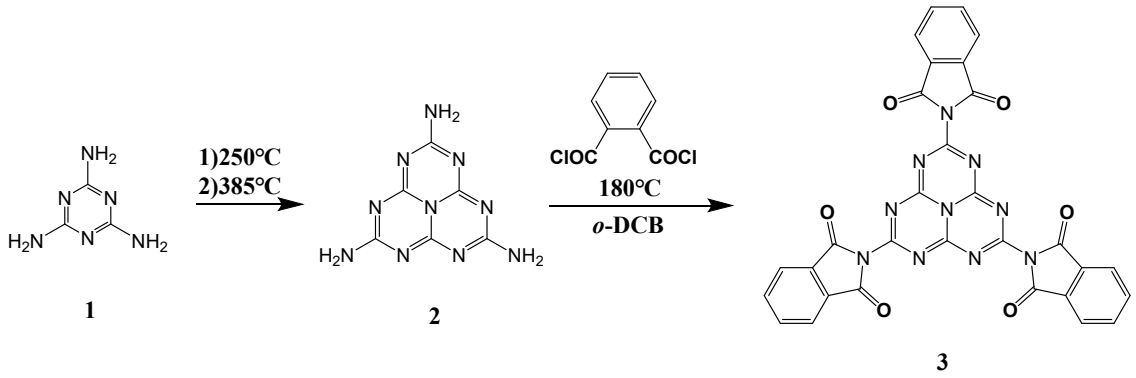

Scheme S1. Synthesis of **2** and **3**.

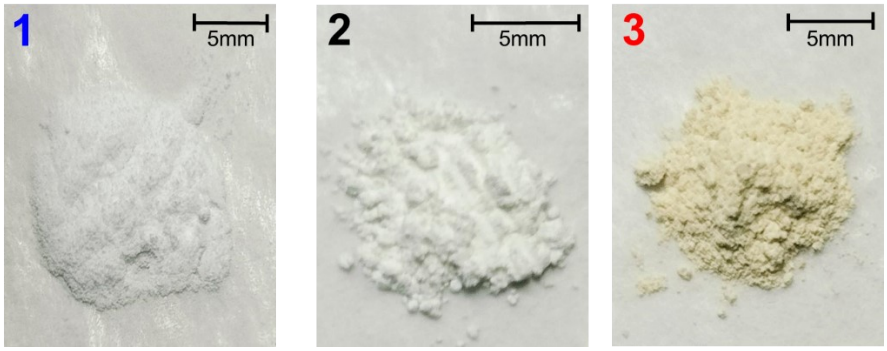

Figure S1. photographic images of **1-3**.

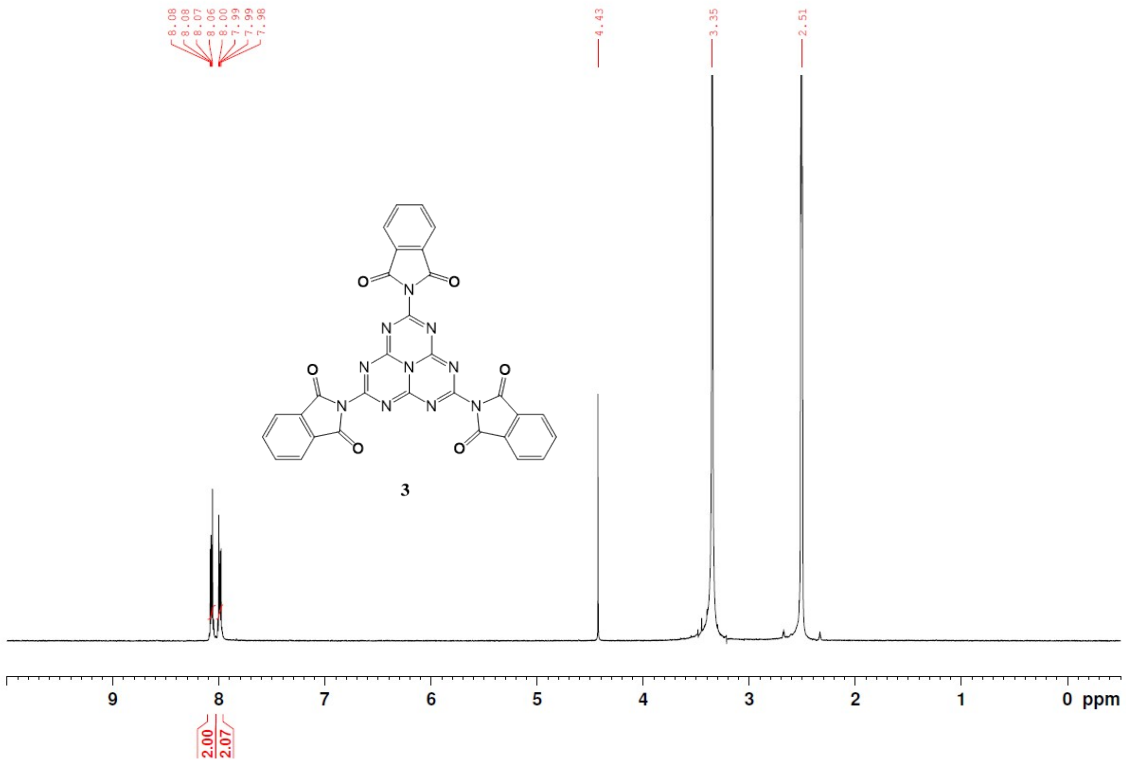

Figure S2. ^{1}H NMR spectrum of compound **3** in DMSO.

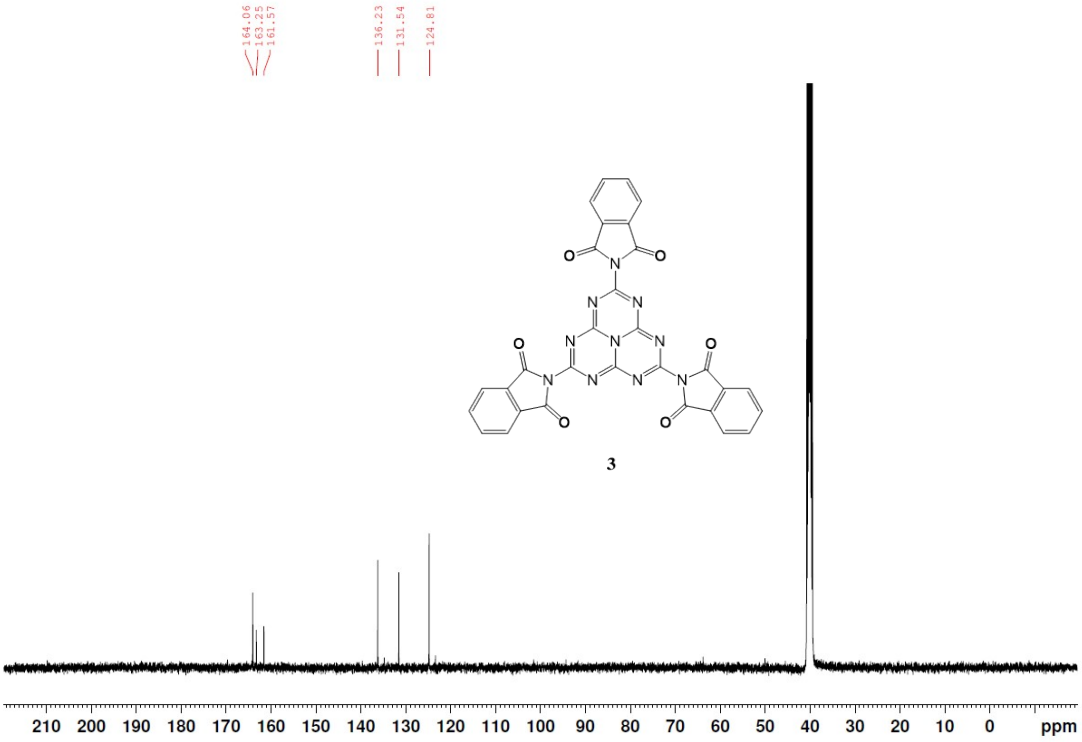

Figure S3. ^{13}C NMR spectrum of compound **3** in DMSO.

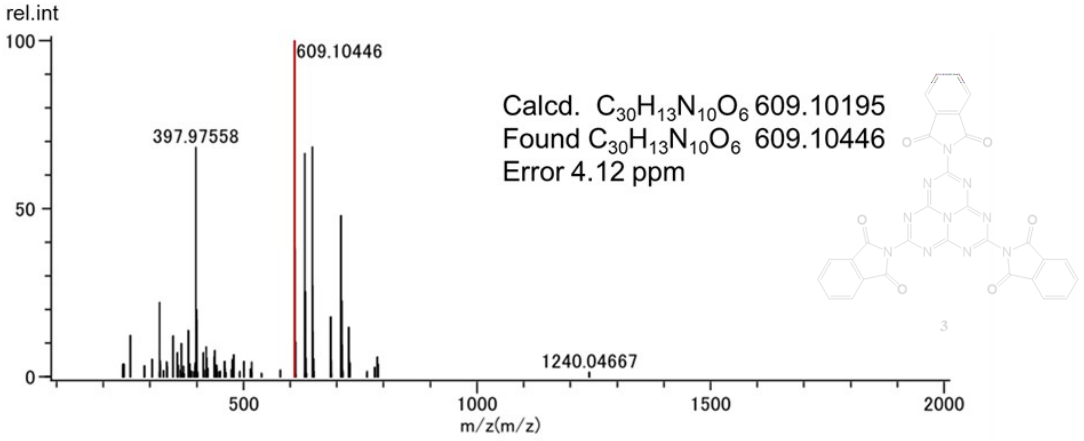

Figure S4. HRESI-MS spectrum of compound **3**.

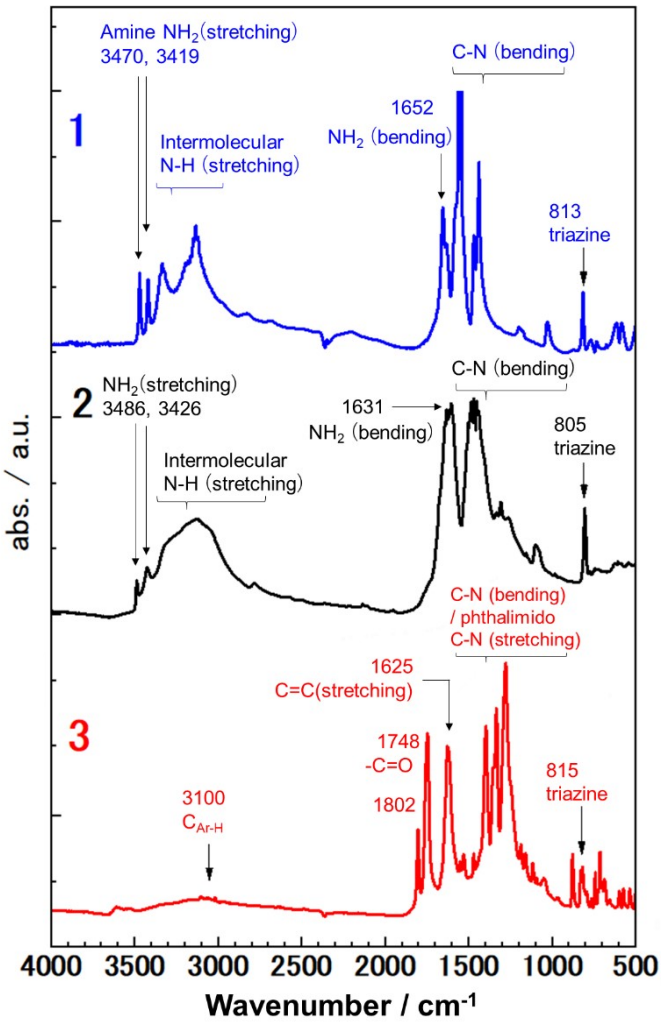

Figure S5. ATR-IR spectra of **1-3.**

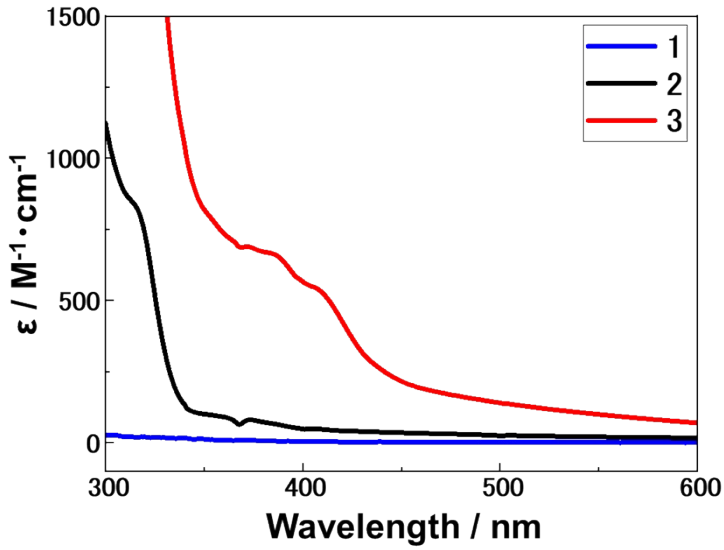

Figure S6. Absorption spectra of **1-3** in DMSO solution.

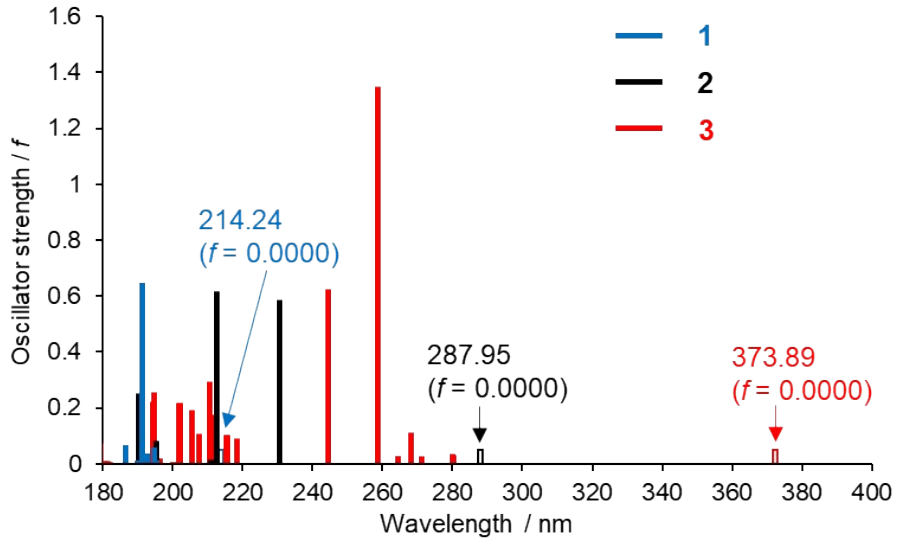

Figure S7. TDDFT generated energy transitions of **1-3**.

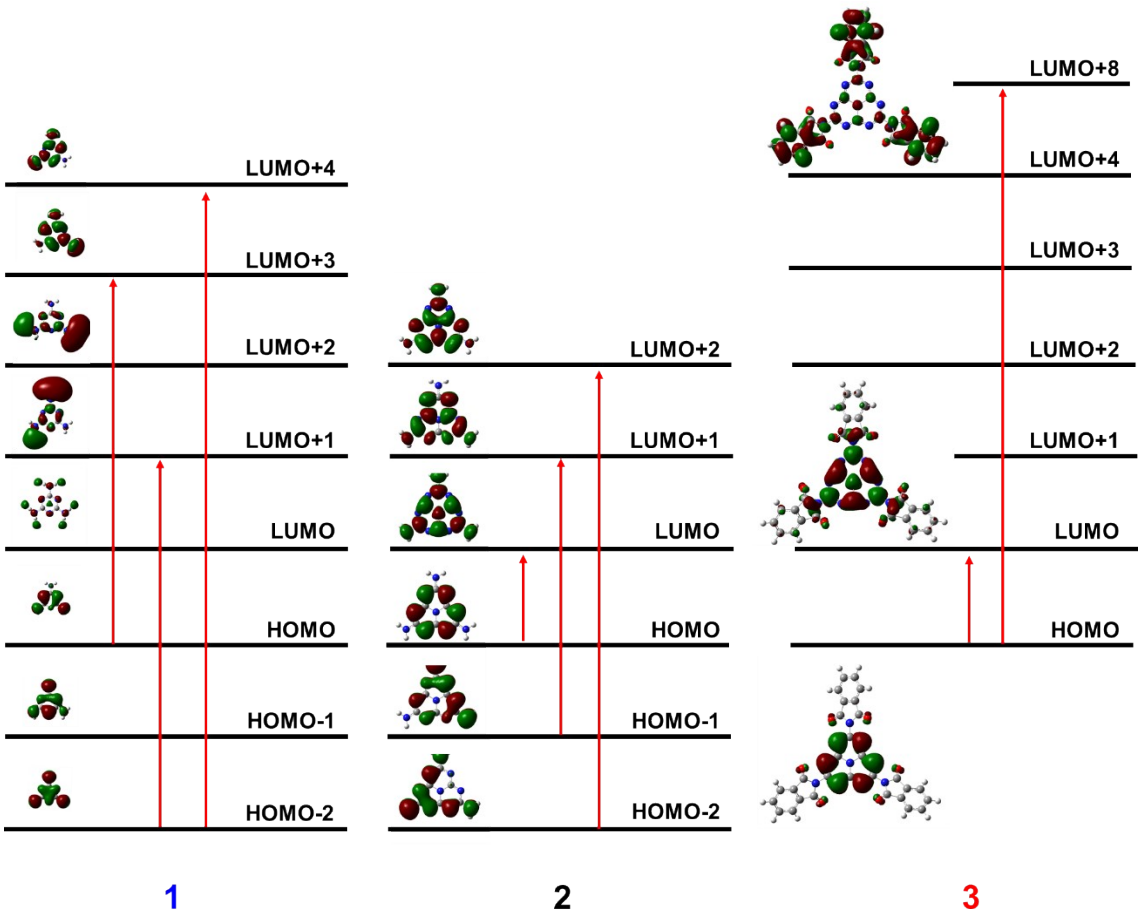

Figure S8. MO for lowest energy transition of **1-3**.

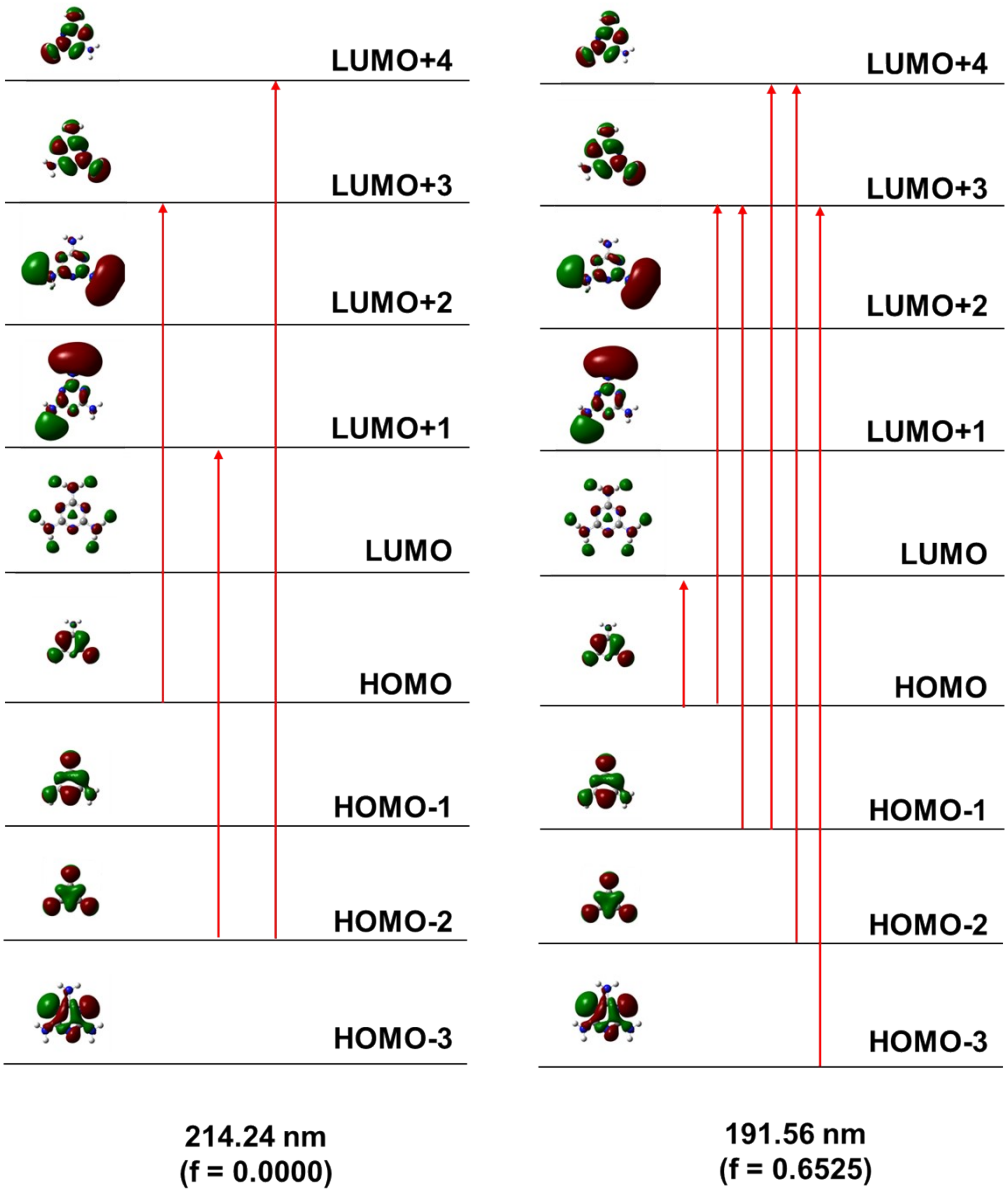

Figure S9. MO for main energy transitions of **1**.

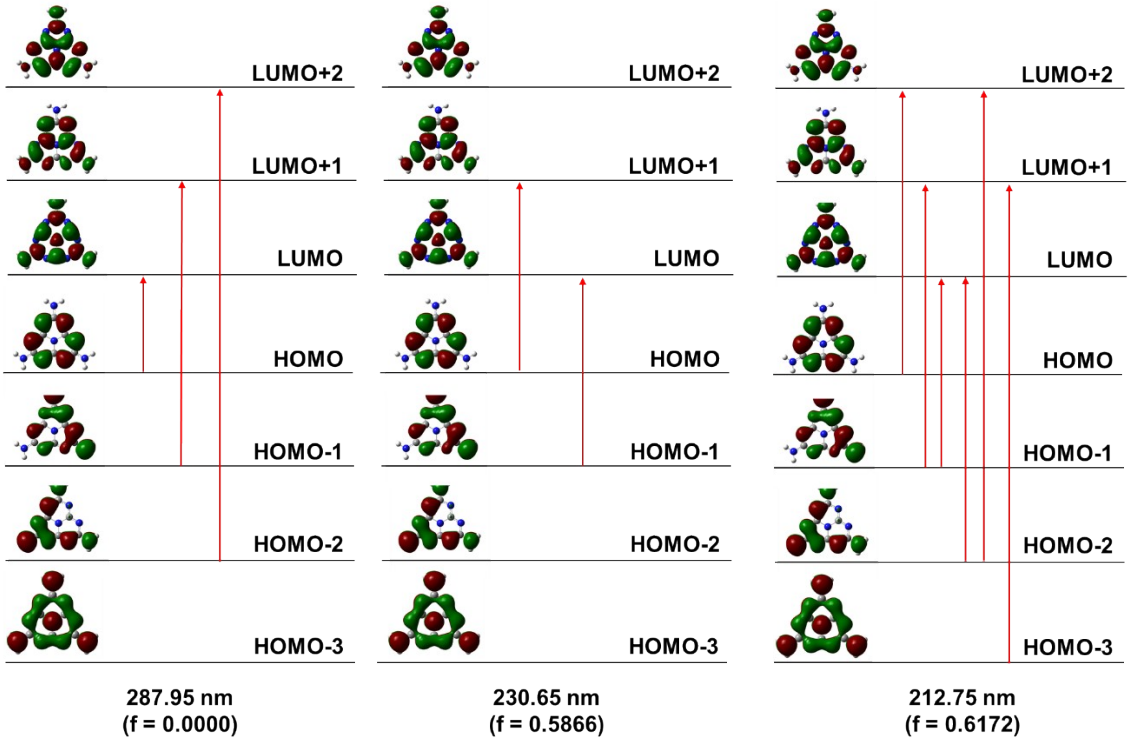

Figure S10. MO for main energy transitions of **2**.

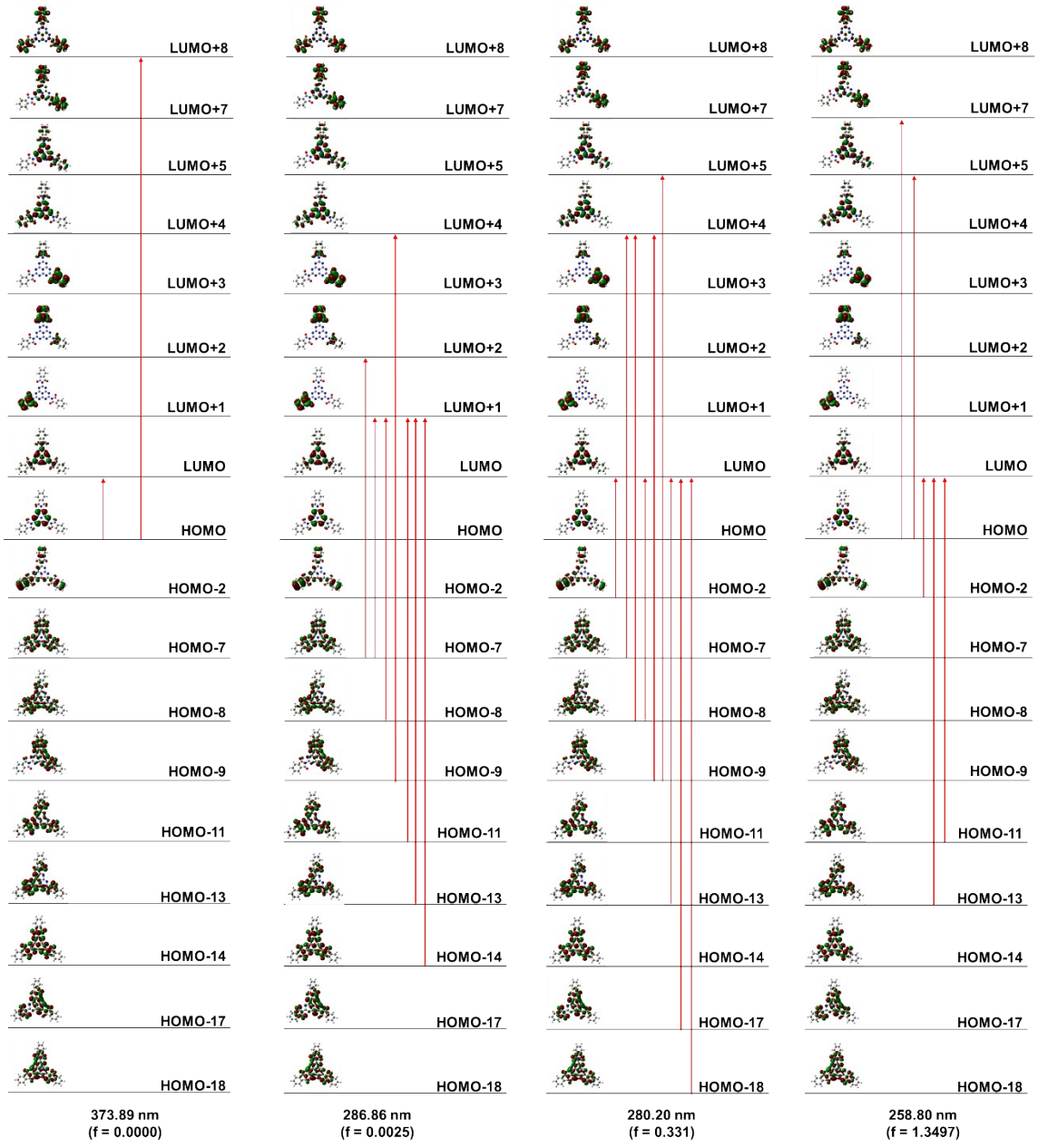

Figure S11. MO for main energy transitions of **3**.

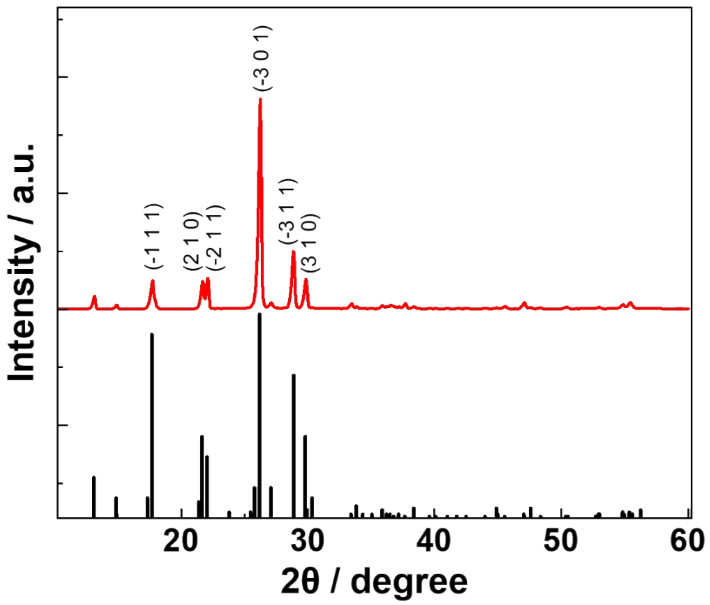

1

Figure S12. XRD patterns of **1.** (Red; experimental, black; reference)

XRD pattern referred from ICDD No.00-024-1654.

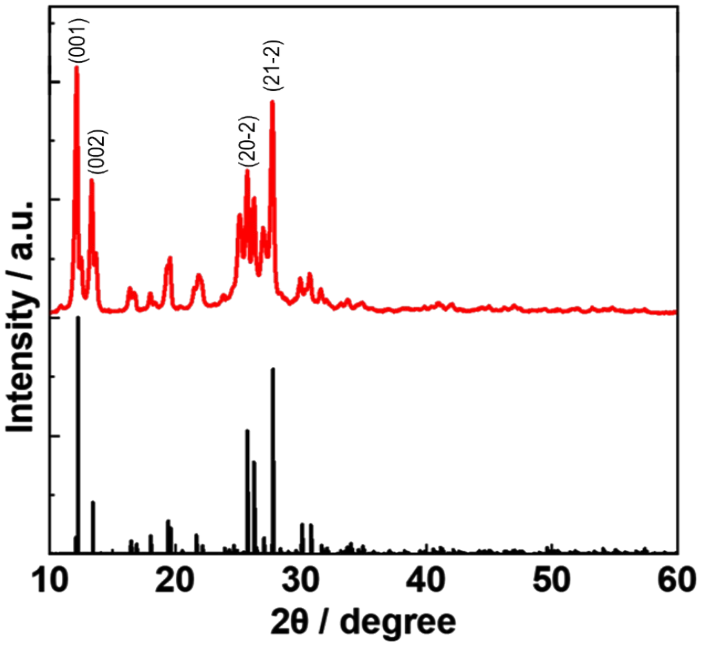

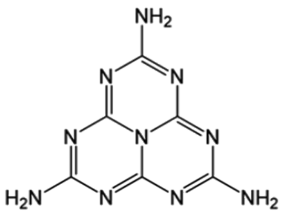

2

Figure S13. XRD patterns of **2.** (Red; experimental, black; simulated)

Simulated XRD pattern of **2** was obtained from CCDC deposition number 639493.

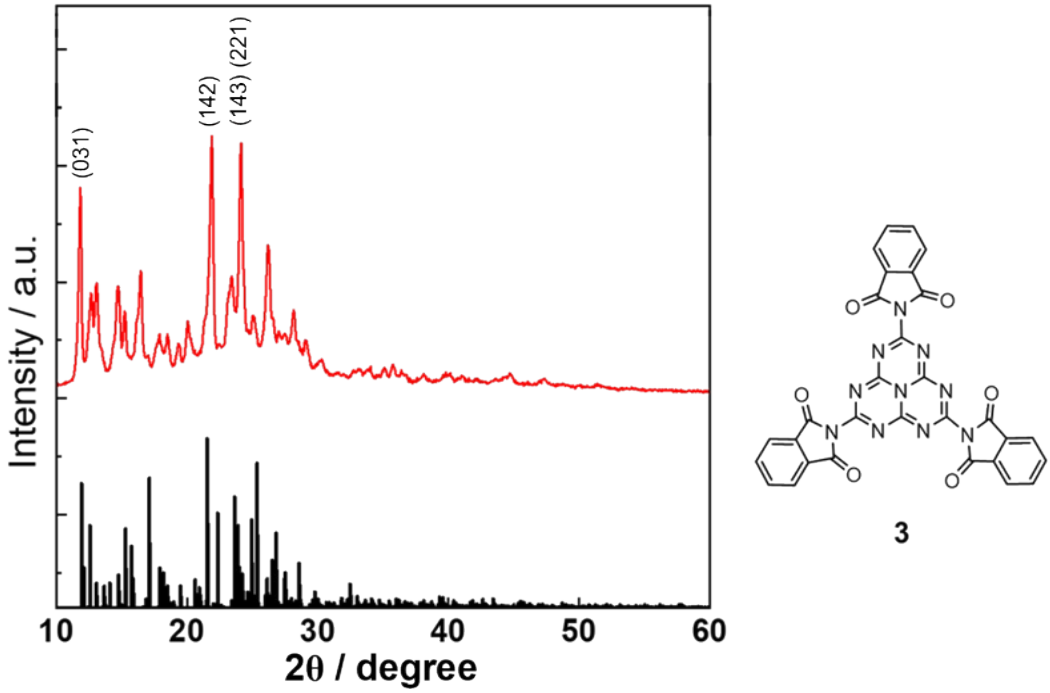

Figure S14. XRD patterns of **3.** (Red; experimental, black; simulated)

Simulated XRD pattern of **3** was obtained from CCDC deposition number 868710.

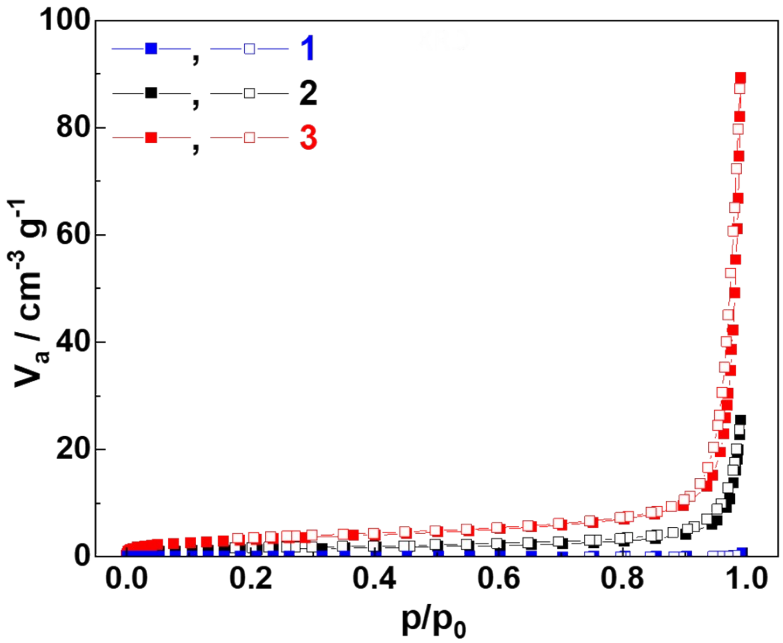

Figure S15. N_2 isotherms of **1-3.** (Adsorption; solid dots, desorption; open square)

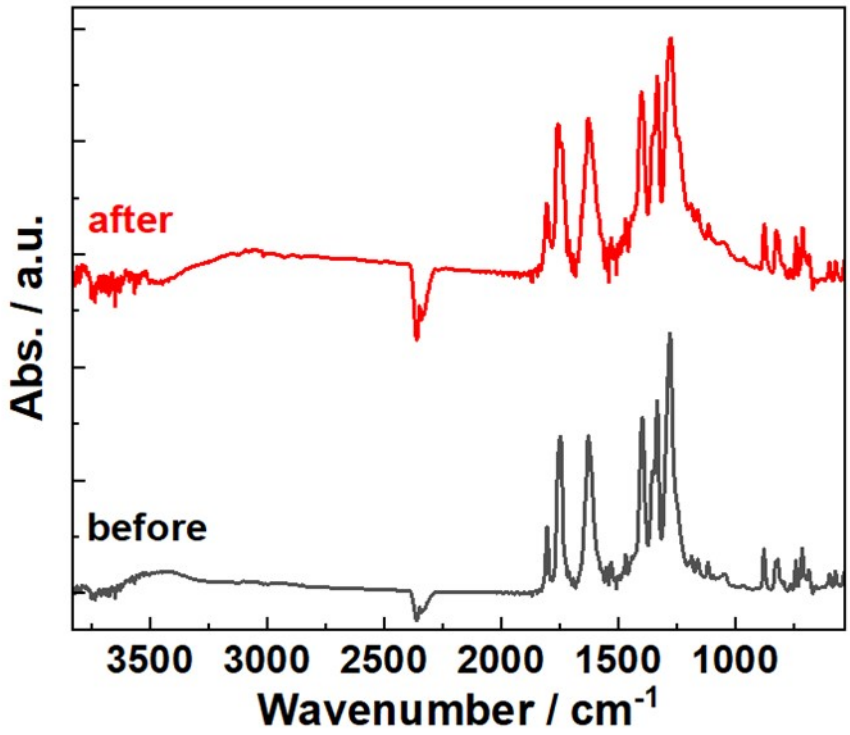

Figure S16. IR spectra of **3** before and after the photocatalytic H_2O_2 production reaction.

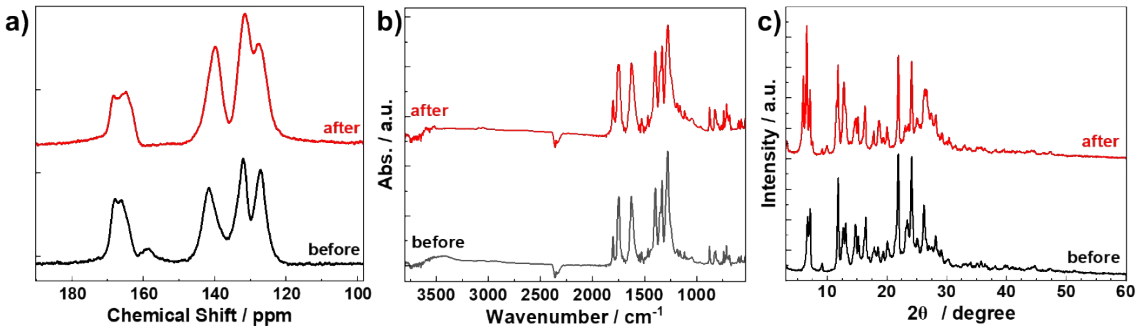

Figure S17. The result of **3** before and after the photocatalytic H_2O_2 production cycle test.
a) solid-state NMR spectra, b) IR spectra, c) XRD pattern

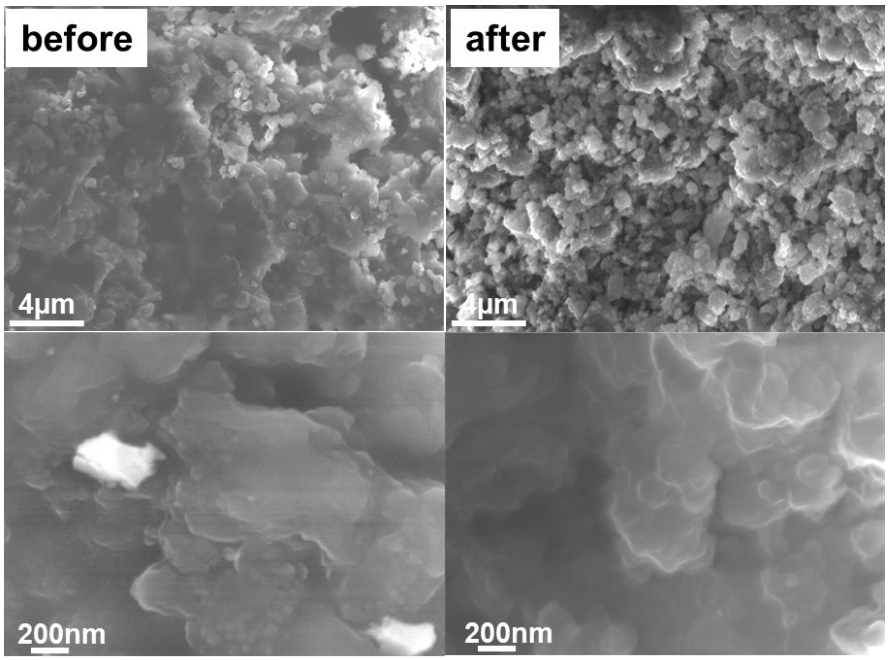

Figure S18. SEM images of **3** before and after the photocatalytic H_2O_2 production cycle test.

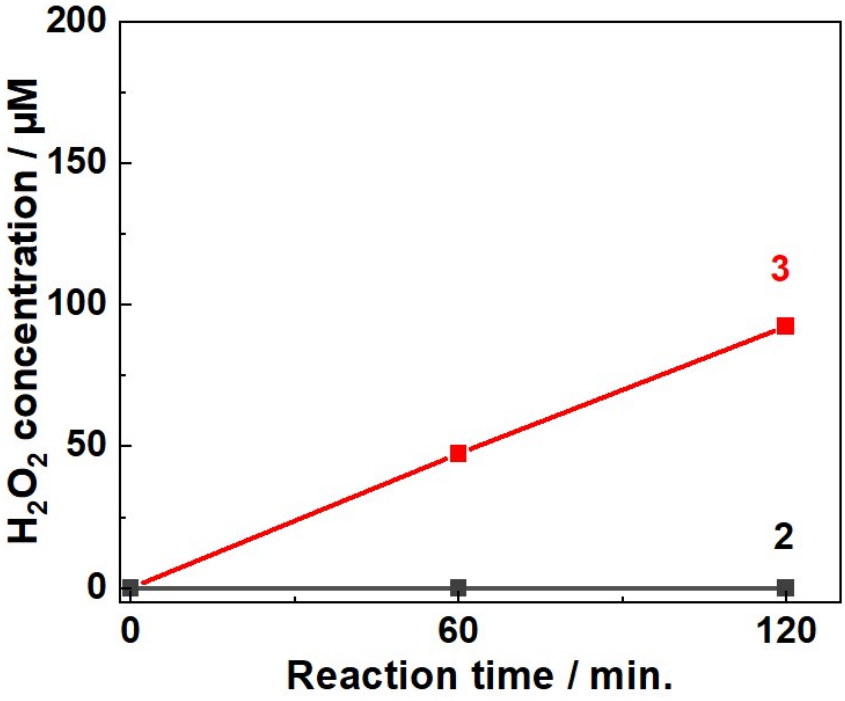

Figure S19. Photocatalytic H_2O_2 production test without ethanol at pH =7 (no sacrificial reagent).

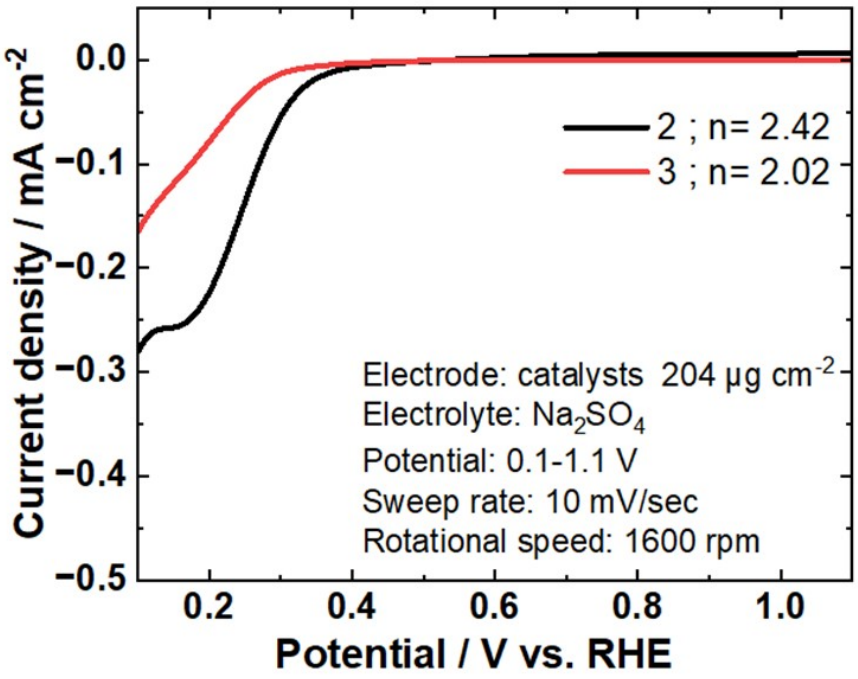

Figure S20. RRDE measurements in O_2-saturated phosphate-buffered 0.1M Na_2SO_4 aqueous.

Table S1. Decomposition of C1s, O1s, and N1s

C 1s - before

Name	C-C/C=C 284.6 eV	C-N 286.0 eV		C=N-C 288.2 eV	$\pi - \pi^*$ 289.7 eV
Peak energy	284.60	286.05		288.16	289.70
FWHM	1.38	1.92		1.47	4.06
Area(%)	38.60	13.01		34.16	14.23

C 1s - after

Name	C-C/C=C 284.6 eV	C-N 286.0 eV	C-O 287.2eV	C=N-C 288.4 eV	$\pi - \pi^*$ 290.0 eV
Peak energy	284.65	286.00	287.20	288.45	290.00
FWHM	1.35	1.92	1.23	1.47	2.47
Area(%)	38.94	12.85	11.36	28.76	8.09

O 1s - before

Name	C=O 531.9 eV	OH 534.7 eV
Peak energy	531.90	534.70
FWHM	2.14	1.89
Area(%)	56.62	43.38

N 1s - before

Name	C=N 398.6 eV	C-N 400.2 eV
Peak energy	398.60	400.20
FWHM	1.42	2.37
Area(%)	52.74	47.26

O 1s - after

Name	C=O 531.9 eV	OH 534.7 eV	C-O 535.2 eV
Peak energy	531.90	534.70	535.62
FWHM	2.40	1.71	0.96
Area(%)	49.38	45.62	4.99

N 1s - after

Name	C=N 398.6 eV	C-N 400.2 eV
Peak energy	398.60	400.20
FWHM	1.38	2.76
Area(%)	38.87	61.13

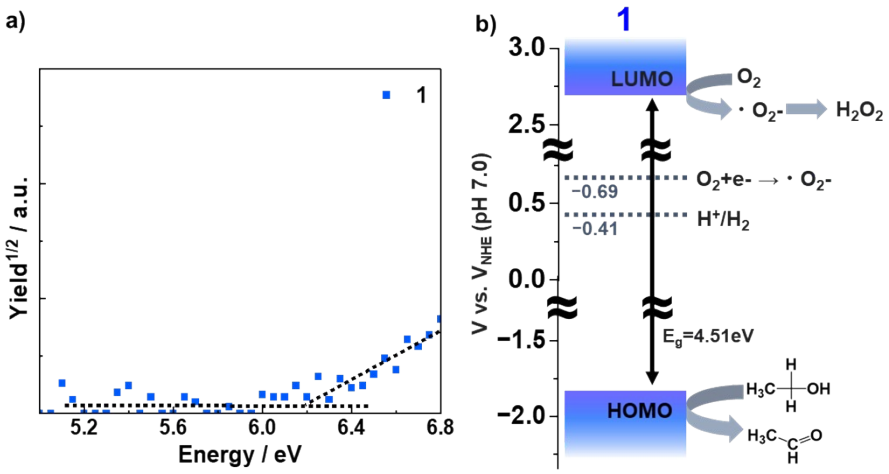

Figure S21. a) PYS of **1,** b) Schematic illustration of the electronic band structure and redox potential alignment (vs. NHE at pH 7.0) of **1**.

The HOMO of **1** was calculated to be -6.24 eV (vs. vacuum). $Gap_{HOMO-LUMO}$ was estimated as 4.51eV from the edge of absorption spectra in Figure 2. From these results, the LUMO of **1** was estimated to be -1.73eV (vs. vacuum), which was corresponding to the HOMO to be +1.80 eV (vs. NHE) and LUMO to be -2.71 eV (vs. NHE).

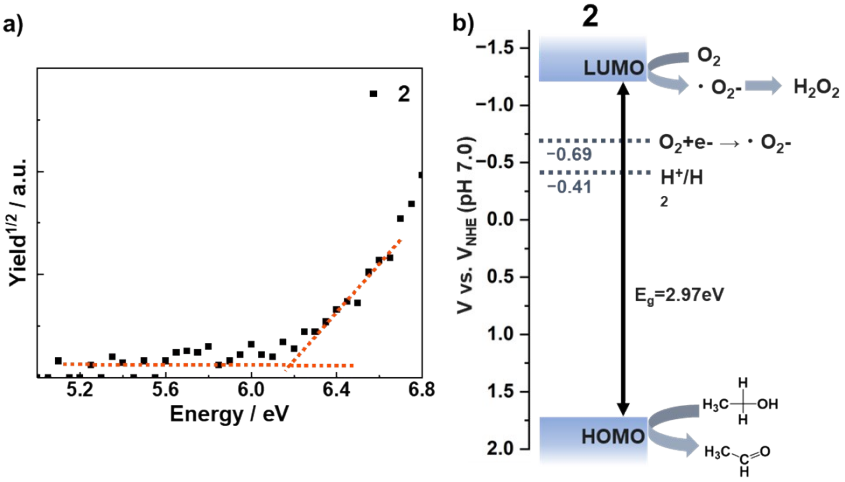

Figure S22. a) PYS of **2**, b) Schematic illustration of the electronic band structure and redox potential alignment (vs. NHE at pH 7.0) of **2**.

The HOMO of **2** was calculated to be -6.18 eV (vs. vacuum). $Gap_{HOMO-LUMO}$ was estimated as 2.97eV from the edge of absorption spectra in Figure 2. From these results, the LUMO of **2** was estimated to be -3.21eV (vs. vacuum), which was corresponding to the HOMO to be +1.74 eV (vs. NHE) and LUMO to be -1.23 eV (vs. NHE).

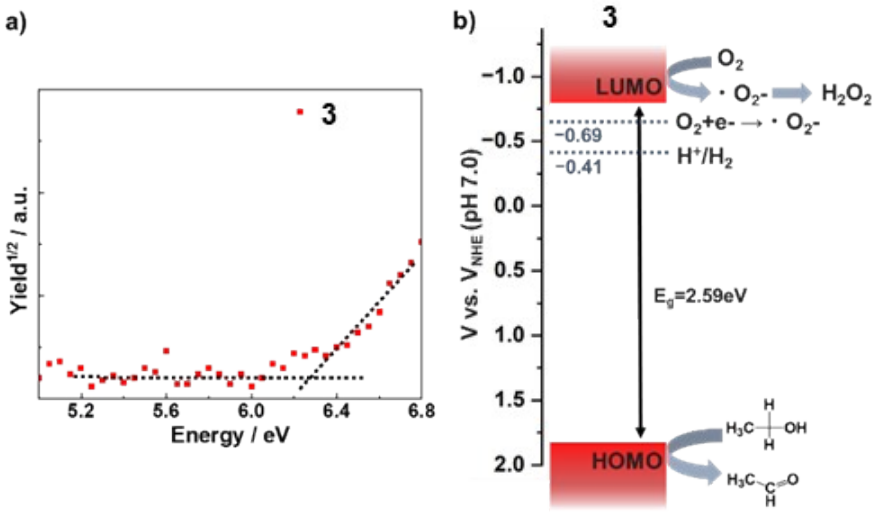

Figure S23. a) PYS of **3**, b) Schematic illustration of the electronic band structure and redox potential alignment (vs. NHE at pH 7.0) of **3**.

The HOMO of **3** was calculated to be -6.26 eV (vs. vacuum). $Gap_{HOMO-LUMO}$ was estimated as 2.59 eV from absorption edge in Figure 2. Therefore, the LUMO of **3** was estimated to be -3.67 eV (vs. vacuum), which was corresponding to the HOMO to be +1.82 eV (vs. NHE) and LUMO to be -0.77 eV (vs NHE).

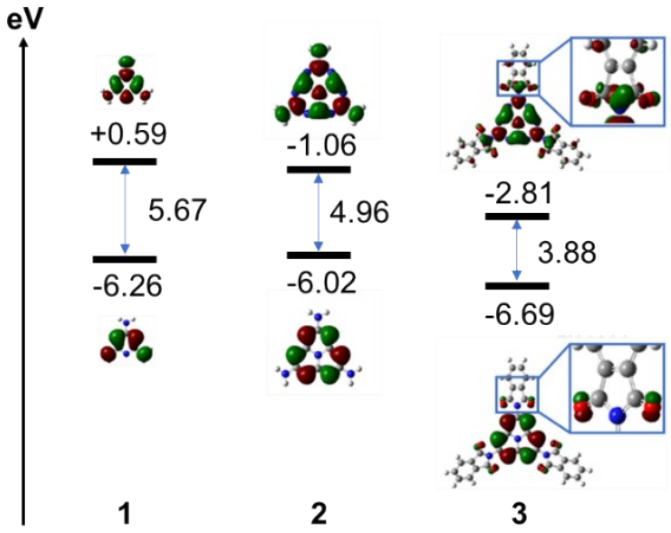

Figure S24. HOMO and LUMO energy diagram of **1-3**.

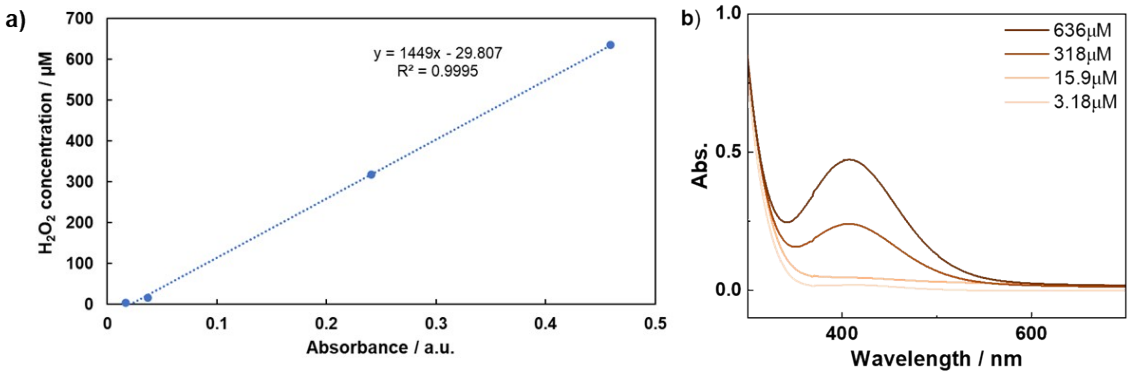

Figure S25. a) Standard calibration curve and b) corresponding spectra for the activity measurements.

Table S2. Summary of H_2O_2 production performance with heptazine-based polymers and molecules with alcohol/O_2 sacrificial conditions.

Sample	**State**	**Condition**	**Light source**	**H_2O_2 [μmol/h·g]**	**Ref.**
C_3N_4	Polymer	10% EtOH / O_2	2kW Xe lamp (λ > 420 nm)	125	[1]
M (C_3N_4 from melamine)	Polymer	10% EtOH / O_2	300 W Xe lamp (> 420 nm)	< 200	[2]
T (C_3N_4 from thiourea)	Polymer	10% EtOH / O_2	300 W Xe lamp (> 420 nm)	< 200	[2]
MT (C_3N_4 from melamine/thiourea)	Polymer	10% EtOH / O_2	300 W Xe lamp (> 420 nm)	250	[2]
KMT (C_3N_4 from KCl/melamine/thiourea)	Polymer	10% EtOH / O_2	300 W Xe lamp (> 420 nm)	600	[2]
AKMT (C_3N_4 from NaOH/melamine/thiourea)	Polymer	10% EtOH / O_2	300 W Xe lamp (> 420 nm)	3600	[2]
KTTCN (K containing C_3N_4)	Polymer	0.5 % IPA / O_2	300 W Xe lamp (λ > 420 nm)	720	[3]
NCNT (3D network of C_3N_4 tube)	Polymer	10% EtOH / O_2	300 W Xe lamp (> 420 nm)	486	[4]
ACN HDMP grafted C_3N_4	Polymer	10% IPA / O_2	300 W Xe lamp (λ > 420 nm)	174	[5]

SS-CN (sulfur doped C_3N_4 nanosheet)	Polymer	10% IPA / O_2	300 W Xe lamp ($\lambda > 420$ nm)	567	[6]
1	**Molecule**	10% EtOH / O_2	300 W Xe lamp	0	[This work]
2	**Molecule**	10% EtOH / O_2	300 W Xe lamp ($\lambda > 390$ nm)	257	[This work]
3	**Molecule**	10% EtOH / O_2	300 W Xe lamp ($\lambda > 390$ nm)	479	[This work]

[1] Y. Shiraishi, S. Kanazawa, Y. Sugano, D. Tsukamoto, H. Sakamoto, S. Ichikawa, T. Hirai, *ACS Catal.* 2014, **4,** 774–780.

[2] P. Zhang, Y. Tong, Y. Liu, J. J. M. Vequizo, H. Sun, C. Yang, A. Yamakata, F. Fan, W. Lin, X. Wang, W. Choi, *Angew. Chem. Int. Ed.*, 2020, **59,** 16209-16217.

[3] J. Zhang, C. Yu, J. Lang, Y. Zhou, B. Zhou, Y. H. Hu, M. Long, *Appl. Catal. B,* 2020, **277,** 119225

[4] X. Yu, C. Hu, D. Hao, G. Liu, R. Xu, X. Zhu, X. Yu, Y. Ma, L. Ma, *Solar RRL*, 2021, **5,** 2000827

[5] Y. Yang, G. Zeng, D. Huang, C. Zhang, D. He, C. Zhou, W. Wang, W. Xiong, X. Li, B. Li, W. Dong, Y. Zhou, *Appl. Catal. B,* 2020, **272,** 118970.

[6] C. Fenga, L. Tanga, Y. Deng, J. Wang, Y. Liu, X. Ouyang, H. Yang, J. Yu, J. Wang, *Appl. Catal. B,* 2021, **281,** 119539.